

HYDROLOGICAL IMPLICATIONS OF CLIMATE CHANGE ON RIVER BASIN WATER CYCLE: CASE STUDIES OF THE YANGTZE RIVER AND YELLOW RIVER BASINS, CHINA

LIU, L.^{1*} – XU, Z. X.²

¹*College of Water Resources and Civil Engineering, China Agricultural University, Center for Agricultural Water Research in China, Beijing 100875, China*

²*College of Water Sciences, Beijing Normal University, Joint Center for Global Change Studies (JCGCS), Beijing 100875, China
(phone: +86-10-62736533; fax: +86-10-62737796)*

**Corresponding author
e-mail: liuliu@cau.edu.cn*

(Received 30th Apr 2017; accepted 25th Jul 2017)

Abstract. As the two largest rivers in China, the Yangtze and Yellow Rivers are of great importance for water cycle and hydrological processes over the country, which have been significantly affected by climate change. In this study, by assessing the suitability of multiple GCMs (General Circulation Models) recommended by IPCC (Intergovernmental Panel on Climate Change), SDSM (Statistical Downscaling Model) and ASD (Automated Statistical Downscaling) were used to generate future climate change scenarios, which were used to drive VIC (Variable Infiltration Capacity) and SWAT (Soil and Water Assessment Tool) models to quantify climate change impacts in the Yangtze River Delta region and upper reaches of the Yellow River basin, respectively. Results showed that suitability assessment method adopted in this study coupled with statistical downscaling could effectively reduce uncertainties of GCMs. Compared with the baseline period (1961-1990), projected annual runoff in future periods (2046-2065 and 2081-2100) would decrease by 9.5% and 3% in the Yangtze River Delta region. While annual runoff in the upper Yellow River basin during future two periods would decrease by 16.9% and 22.2%. The results are of great significance to future water resources management and sustainable development under climate change in major river basins of China.

Keywords: *statistical downscaling, distributed hydrological model, changing environment, scenario analysis, Tibetan Plateau*

Introduction

The Fifth Assessment Report (AR5) of the Intergovernmental Panel on Climate Change (IPCC) pointed out that climate change has become an indisputable fact that will greatly threaten global and local water resource security (Stocker et al., 2013). In China, the tendency of climate change has been generally consistent with its global pattern (Qin, 2003; Qin et al., 2007). The multiscale, all-dimension, multi-level influences of climate change on humans, the ecology and environment (Hadson and Jones, 2002; Varis et al., 2004; Burn et al., 2010; Elfert and Bormann, 2010; Karamouz et al., 2011; Jung and Chang, 2011; Marvel and Bonfils, 2013; Jeong et al., 2014; Xu et al., 2015) are key risk factors for global sustainable development. Because the water cycle connects humans, the ecology and environment, its response to future climate change has become a focus of scientists, the general public, and decision-makers all over the world.

China has a vast territory and various climate types. Because of substantial differences in geological environment, climate, and economic development stages in various regions, the influences of climate change vary. In the context of global warming, the frequency and intensity of climate extremes such as high temperature, low temperature, heavy precipitation and droughts in China had varying tendencies and regional differences (Piao et al., 2010). Recently, a number of researchers have conducted extensive studies of climate change and its effects on water resources in China. In general, it was found that over the past 100 years, hydrological climate elements changed substantially in major basins of the country, showing substantial temperature rises in most areas. In the last 50 years, there has been an uneven south-north precipitation distribution in the eastern monsoon region (Ye and Huang, 1996; Fu et al., 2005; Ding and Ren, 2008; Ding et al., 2006) and reduced basin runoff in the majority of northern exorheic rivers, aggravating water resource supply-demand conflicts in the north and pressure for flood control in the south (Chen, 2002; Liu, 2004; Qian et al., 2007). In most regions of the country, the potential (water surface) evaporation capability decreased dramatically (Qiu et al., 2003; Yang et al., 2003; Liu et al., 2004; Ren and Guo, 2006). Future climate change might exert strong impacts on water resources in China (Wang et al., 2002; Liu, 2007; Zhang and Liu, 2000; Xia et al., 2008), with reduced runoff in northern rivers but increased runoff in southern ones (Lin et al., 2006). Annual average evaporation may be on the rise (Wang et al., 2003), as may be the case also for the frequency of flood and drought disasters, which would further increase the vulnerability of water resources and conflict between water supply and demand (Lin et al., 2006).

Because of water cycle and water resources pattern changes in major river basins of China and prominent water issues such as flood disasters in the south and water shortages in the north, it is of great scientific importance and value to study the mechanism and spatiotemporal variation of the continental water cycle under the background of climate change. This will help assess the influence of such change on the basin water cycle and ensure sustainable socioeconomic development in the country.

In the current study, the Yangtze River Delta region and the upper reaches of Yellow River basin were selected to represent typical southern and northern basins in China. A multi-criteria score-based method was used to assess the suitability of multiple General Circulation Models (GCMs) provided by the IPCC. Screened GCM output results were downscaled to create future climate change scenarios suitable for the Yangtze and Yellow River basins. These scenarios were used to drive distributed hydrological models to simulate the spatiotemporal variation of water cycle elements in the study area, thereby evaluating the response of the river basin water cycle to future climate change.

Materials and Methods

Study area

The Yangtze is the longest river in Asia and the third longest in the world with a length of over 6300 km. Its drainage area, the Yangtze River basin, is located between 24°30'-35°45'N and 90°33'-122°25'E, spanning a total area of $\sim 1.8 \times 10^6$ km². The Yangtze River basin stretches from the eastern Tibetan Plateau to the East China Sea and crosses 19 provinces in China (*Fig. 1*). The economy of the Yangtze River basin contributes 41.1% of China's gross domestic product, and the area supports 34% of the nation's population (Xu and Ma, 2009). Most of the YRB belongs to the East Asian

monsoon region, which is sensitive and vulnerable to climate change (Fang et al., 2010; Xu and Ma, 2009). Human-induced land use/land cover change and climate change are now having enormous impacts on its water cycle (Zhang et al., 2014).

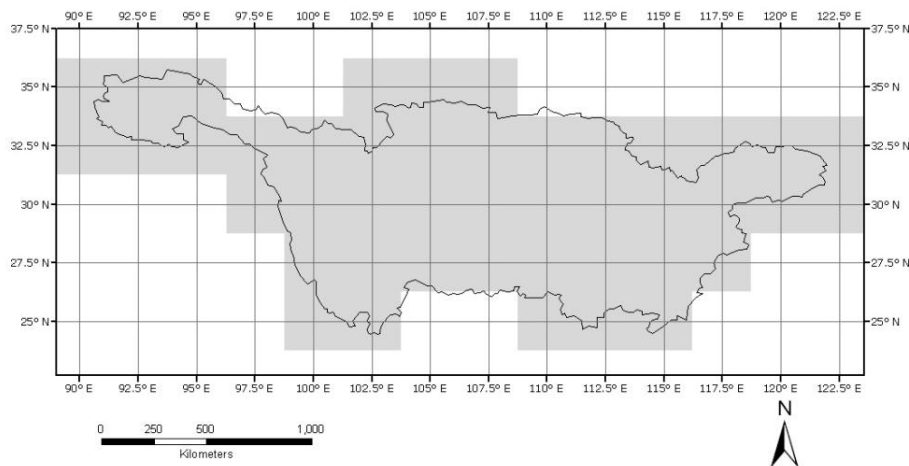


Figure 1. Geographical boundary of Yangtze River basin with grids distribution used for GCMs

The Yellow River is the second largest river in China with a drainage area of $7.95 \times 10^5 \text{ km}^2$ (Fig. 2), and its topography is highest in the west and the lowest in the eastern parts of the Yellow River basin. The basin is located at mid-latitudes with a different climate prevailing in the southeastern part (higher precipitation) as compared to the northwestern part (lower precipitation). In addition, 91.93% of the total land has been utilized for vegetative cover in the basin. Due to climate change and intensifying human activities, particularly increasing human withdrawal of water for agriculture irrigation, streamflow in the Yellow River has significantly decreased since 1980s (Li et al., 2017; Zhang et al., 2009).

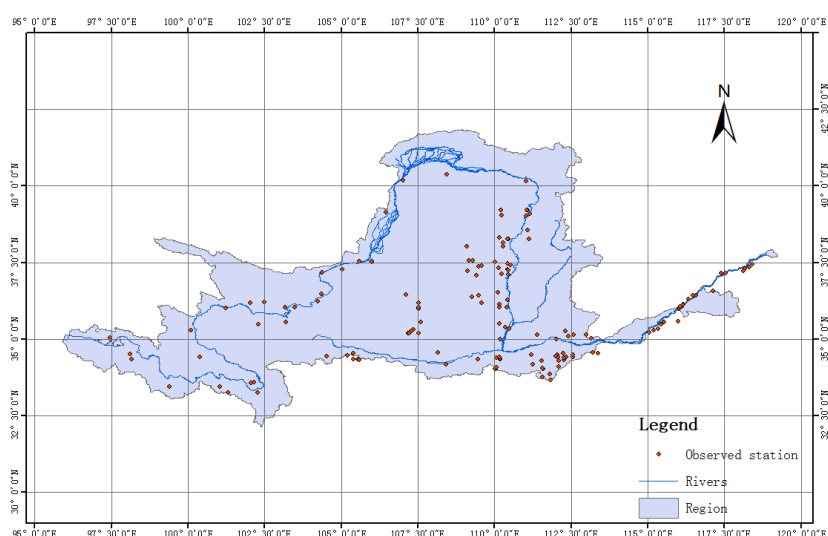


Figure 2. Geographical boundary of Yellow River basin with grids distribution used for GCMs

GCM suitability assessment method

Taking the degree of fit of statistical values from GCM output and those from field-measured data as objective functions, the performance of each such function was scored, thereby evaluating the comprehensive performance of GCMs.

The mean value, coefficient of variability (= standard deviation / mean value), and normalized root mean square error (NRMSE) were used to characterize closeness between the mean value and deviation of GCM output variables and those of measured variables. NRMSE was defined as the ratio of root mean square error to the corresponding standard deviation.

Pearson correlation coefficients in both chronological (multiyear average monthly sequence) and spatial (mean value of climate elements at stations) sequences were used to characterize the closeness between GCM simulation and measured values, thereby evaluating the simulated variables' intraannual change and spatial degree of fit.

The rank-based nonparametric Mann-Kendall method was used to detect long-term tendencies (MK Zc) and magnitudes (MK Slope) of every variable. If areas where the MK Zc of GCM output variables matched measured values did not reach 95%, MK Slope was not included in the scoring.

Empirical orthogonal functions (EOFs) were used to qualitatively and quantitatively characterize variable spatiotemporal variation. Preliminary analysis showed that the first and second EOF characteristic vectors of nearly 20 variables were able to explain most of the deviations. Hence, these two vectors were included in rank scoring.

Two statistics of the probability density function, Brier score (BS) and skill score (Sscore), were used to evaluate the effectiveness of GCM simulation of that function. BS is the mean square deviation of probabilistic prediction, and Sscore is used to describe the overlap between the computed and measured probability distribution.

A total of 11 statistics were included, i.e., mean, coefficient of variability, NRMSE, temporal correlation coefficient, spatial correlation coefficient, trend analysis rank statistics, trend analysis variation magnitude, first and second EOF characteristic vectors, and BS and Sscore of the probability density function. Performance of each of the statistics was considered as one of the objective functions. A multi-criteria rank score (RS) value was computed for every objective function by assigning a value of 0-10, based on GCM performance. The calculation was:

$$RS_i = \frac{x_i - x_{\min}}{x_{\max} - x_{\min}} * 10, x_i < x_{\max} \quad (\text{Eq.1})$$

where x_i is relative error in a statistic between simulated and measured values. The smaller the value is, the lower the score is. For a specific GCM output variable, the final total score was calculated by averaging the scores of all statistics. The better the simulation results, the lower the score. The score represents the degree of fit between GCMs outputs and measured values. It could be used to compare and analyze different GCMs, but it does not indicate the actual simulation accuracy of a given GCM.

Downscaling model

The Statistical Downscaling Model (SDSM) has both of deterministic transfer functions and stochastic components (Wilby et al., 2002). It has been widely applied in the statistical downscaling studies for both climate variables and air quality variables, and

has been recommended by the Canadian Climate Impacts and Scenarios (CCIS) project (<http://www.cics.uvic.ca>).

An automated regression-based statistical downscaling model (ASD) (Hessami et al., 2008), inspired by the existing SDSM was developed within the Matlab environment, which is an easy to use graphical user interface for the statistical downscaling of GCM outputs to regional or local variables and already been successfully applied in major river basins of the east monsoon region in China (Xu et al., 2013).

Distributed hydrological models

The Taihu basin, located in the Yangtze River Delta region, is selected as the typical area for hydrological modeling in this study, which is characterized by a flat terrain, a complex river network, and various polder areas, without a clear outlet. Based on a 90-m DEM, it is difficult to extract the basin river network and simulate runoff yield and concentration over the entire basin. Therefore, the distributed Variable Infiltration Capacity (VIC) model based on grids was used to directly obtain gridded runoff depth in the basin. The VIC model considers physical exchange processes of atmosphere-vegetation-soil, primarily reflected by the variation of water and heat conditions and water and heat transfer in those three components. The model has been widely used to study the effects of climate change on hydrologic processes (Yuan et al., 2005; Liu, 2004; Su and Xie, 2003; Lohmann et al., 1998; Nijssen et al., 1997; Abdulla et al., 1996). VIC can either simultaneously simulate atmospheric-hydrological energy balance and water balance, or just calculate water balance, export runoff depth, and evaporation at each grid. Through a runoff concentration model, it transforms grid runoff depth into water flow at the basin outlet, eliminating the shortcomings of traditional hydrological models in the description of thermal processes.

The upper reaches of the Yellow River basin were selected to investigate the influences of climate change on the basin water cycle in this study. The reasons for this selection were: (1) The upper reaches are the origin of the Yellow River, and runoff variation there affects the entire basin; (2) future runoff change in the upper reaches can be used to validate basin-wide runoff change; (3) results of sub-basin estimation can provide accurate and detailed information for future runoff variation tendencies. In the upper reaches of the Yellow River basin, there is strong terrain fluctuation, an extractable river network, and abundant hydrologic data for the basin outlet. The Soil and Water Assessment Tool (SWAT) model (Arnold et al., 1998; Neitsch et al., 2005) was used for distributed hydrological simulation. Parameter sensitivity was analyzed by use of the built-in sensitivity analysis module.

Dataset

To include as many GCMs as possible from different countries and ensure the integrity and reliability of GCM outputs, 23 GCMs recommended by the IPCC were selected (*Table 1*). Monthly series including 15 climate variables, i.e., average temperature, relative humidity, longitudinal and latitudinal wind speeds, geopotential heights at the 500, 700 and 850 hPa levels, and two surface climate variables (temperature and precipitation) were used in this study. All data were from the IPCC data center. Details of the GCMs are on the website <http://ipcc-ddc.cru.uea.ac.uk>. All GCM output data were normalized to $2.5^{\circ} \times 2.5^{\circ}$ by interpolation. Data series were from the period 1950 to 1999/2000.

Table 1. Information on GCMs

GCMs	Abbreviation	Developing research institute	Country	Resolution	Period
BCCR:BCM20	BCCR	Bjerknes Centre for Climate Research	Norway	1.9° × 1.9°	1961-2000
PCM	PCM	National Center for Atmospheric Research	United States	2.8° × 2.8°	1961-1999
CCSM3	CCSM3	National Center for Atmospheric Research	United States	1.4° × 1.4°	1961-2000
CGCM2.3.2	MRI	Meteorological Research Institute	Japan	2.8° × 2.8°	1961-2000
CGCM3.1_T47	CGCM47	Canadian Centre for Climate Modelling and Analysis	Canada	2.8° × 2.8°	1961-2000
CGCM3.1_T63	CGCM63			1.9° × 1.9°	1961-2000
CNRM:CM3	CNRM	National Centre for Meteorological Research	France	1.9° × 1.9°	1961-1999
CSIRO:MK30	CSIRO30	Atmosphere Research, Commonwealth Scientific and Industrial Research Organization	Australia	1.9° × 1.9°	1961-2000
CSIRO:MK35	CSIRO35			1.9° × 1.9°	1961-2000
ECHAM4	ECHAM4	Meteorological Research Center	Germany	2.8° × 2.8°	1961-2000
ECHAM5	ECHAM5	Max Planck Institute für Meteorologie		1.9° × 1.9°	1961-2000
FGOALS:g10	FGOALS	State Key Laboratory of Numerical Modeling for Atmospheric Sciences and Geophysical Fluid Dynamics (LASG) / Institute of Atmospheric Physics	China	2.8° × 2.8°	1961-1999
GFDL:CM20	GFDL20	U.S. Department of Commerce / National Oceanic and Atmospheric Administration / Geophysical Fluid Dynamics Laboratory	United States	2.0° × 2.5°	1961-2000
GFDL:CM21	GFDL21			2.0° × 2.5°	1961-2000
GISS:AOM	GISSAOM	National Aeronautics and Space Administration (NASA) / Goddard Institute for Space Studies (GISS)	United States	3° × 4°	1961-2000
GISS:EH	GISSSEH			4° × 5°	1961-2000
GISS:ER	GISSER			4° × 5°	1961-2000
HadCM3	HadCM3	Met Office Hadley Centre for Climate Science and Services	United Kingdom	2.5° × 3.75°	1961-1999
HadGEM1	HadGEM1			1.3° × 1.9°	1961-1999
INM:CM30	INM	College of Computational Mathematics	Russia	4° × 5°	1961-2000
IPSL:CM4	IPSL	Pierre-Simon marquis de Laplace	France	2.5° × 3.75°	1961-2000
MIROC3.2_hires	MIROC-h	Climate System Research Center, Tokyo University; National Environment Research Institute; Frontier Research Center for Global Change (JAMSTEC)	Japan	1.1° × 1.1°	1961-2000
MIROC3.2_medres	MIROC-m			2.8° × 2.8°	1961-2000

ERA-40 and NCEP reanalysis data were taken as the measured data of the meteorological variables to assess the suitability of GCM outputs. Gridded data of monthly average temperature and monthly precipitation from the China Meteorological Administration (<http://ncc.cma.gov.cn>) were used, which were resampled to 2.5° × 2.5° grids.

Results and Discussion

GCM suitability assessment results

The Yangtze River basin

Comprehensive assessment results indicate that FGOALS, ECHAM4, ECHAM5, HadCM3, HadGEM1 and MRI had better performance in the Yangtze River basin than other GCMs (Fig. 3). Zhang et al. (2005) investigated spatiotemporal and circulation characteristics of the water vapor budget in the basin, and emphasized the influence of latitudinal water vapor transport originating from the Bay of Bengal on basin relative humidity. The simulation results of longitudinal and latitudinal wind speed strongly affected the spatiotemporal distribution of basin relative humidity. In the present study, four GCMs that effectively simulated relative humidity (ECHAM4, FGOALS, HadCM3 and HadGEM1) also showed good simulation of longitudinal and latitudinal wind speeds, consistent with previous studies. Temperature simulation results were better than other variables (including relative humidity), also demonstrated in previous studies. Xu et al. (2002) simulated climate change in East Asia based on five climate models, including temperature, precipitation, diurnal range and water vapor data. Their assessment results indicated that ECHAM4 and HadCM2 had best performance in China. In the present study, these two models also demonstrated promising outcomes. However, during

assessment of GCM suitability in the Murray-Darling Basin of Australia, Maxino et al. (2008) obtained larger GCM-computed values of temperature than measured values for most GCMs. In contrast, in an assessment of GCM suitability in the Yellow River basin by Cao et al. (2009) the computed temperature was consistently cooler. In the present study, the computed temperature was warmer in most GCMs than measured. This might have resulted from a large difference of regional climate and circulation characteristics in the basins, as well as different GCM responses to climate characteristic variation (Xu et al., 2015; Miao et al., 2016). Therefore, it is necessary to assess GCM suitability across different basins.

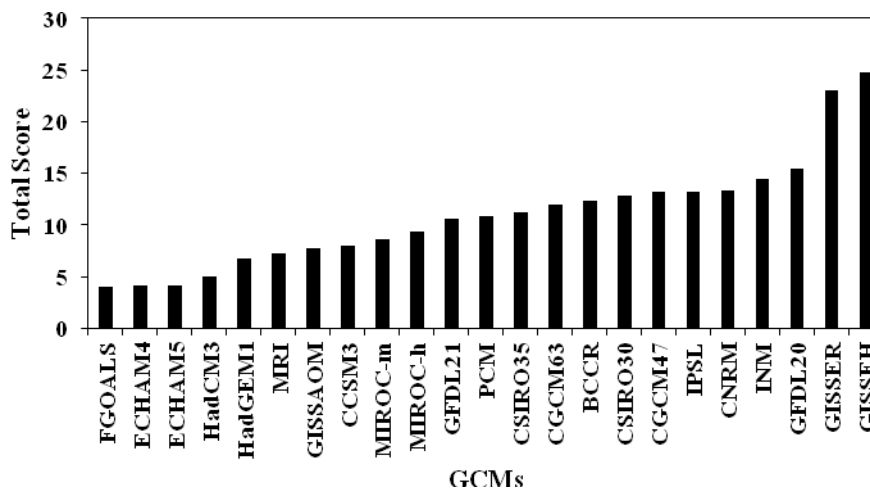


Figure 3. Comprehensive scoring of GCMs in Yangtze River basin

Specifically, we chose the Taihu basin to investigate the influences of climate change on the water cycle in the Yangtze River basin and evaluate GCM suitability. This basin is in the southern Yangtze River Delta. Associated administrative regions include southern Jiangsu, Jiaying, Huzhou, part of Hangzhou in Zhejiang, and most of Shanghai, one of the most economically developed and populated regions in China. The basin water cycle is extremely sensitive to climate change.

Fig. 4 shows RS scores in increasing order. The lower the score is, the better the GCM performance for climate simulation is. Thus, it is seen that the BCCR model had the best performance overall. Therefore, it was used to assess the impacts of climate change. The simulated daily climate data were exported to the A1B scenario including two components, the current period (1961-2000, 20c3m scenario) and future periods (2046-2065 and 2081-2100). A1B is characterized by balanced economic development and greenhouse gas emissions, and is therefore suitable for future planning of coordinated water-economic-environment development in the Taihu basin.

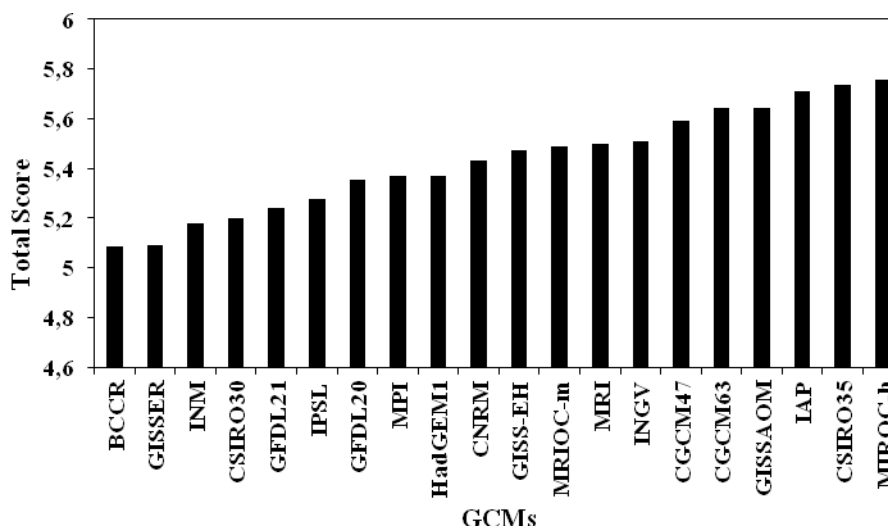


Figure 4. Comprehensive scoring of GCMs in Taihu basin

The Yellow River basin

25 grids of GCM data over the Yellow River basin were selected (Fig. 2). All GCM data were interpolated to a resolution of $2.5^{\circ} \times 2.5^{\circ}$. The comprehensive results showed that the top ten climate models were the MRI, HadGEM1, INM, CSIRO30, MIROC-M, HadCM3, BCCR, GFDL20, CGCM47, and GFDL21 (Fig. 5).

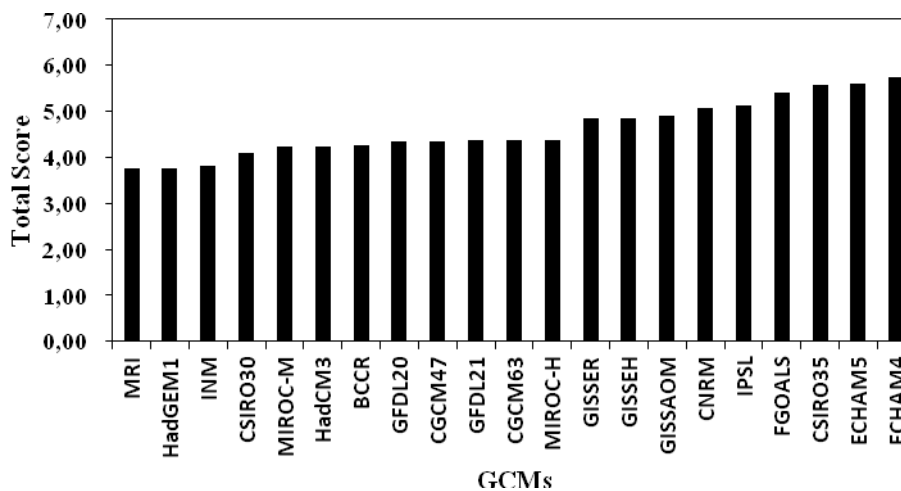


Figure 5. Comprehensive scoring of GCMs in Yellow River basin

While studying summer water vapor transport in the Asian monsoon zone and effects on precipitation in China, Zhou et al. (2008) observed the important role of longitudinal and latitudinal water vapor transport by the Indian monsoon to relative humidity of the basin in China. Also, it was reported that relative humidity was to a large extent affected by the simulation performance of longitudinal and latitudinal wind speeds. In the present study, the GCMs with favorable simulation of relative humidity (MRI, HadGEM1 and

GFDL20) also showed good performance in simulation of those wind speeds. This is consistent with the finds of Zhou et al. (2008).

To analyze uncertainty caused by multiple GCMs and different scenarios and comprehensively consider the consistency and integrity of scenario data in different models, we compared A2 and B1 scenario data in MRI, CSIRO30 and INM, which had the best performance in the Yellow River basin.

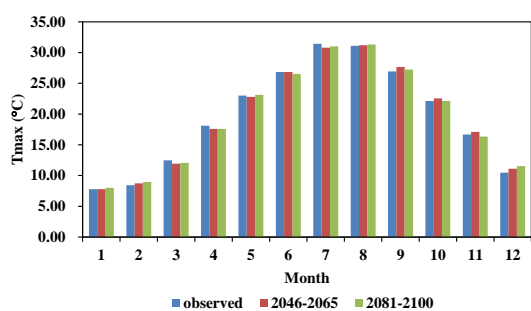
Impacts of climate change on water cycle

The Yangtze River basin

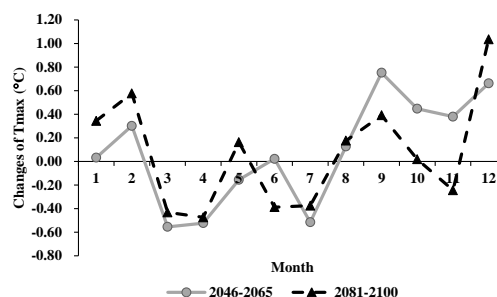
Construction of future climate change scenario

In a previous study by the authors (Chu et al., 2012), we conducted a comparison of statistical downscaling models for the Taihu basin. Specifically, the SDSM and ASD model were used to construct future climate change scenarios for that basin. The results indicated that ASD optimized the selection of predictors, and the simulation results were superior to those of SDSM. Therefore, the ASD model was used herein to construct future climate change scenarios.

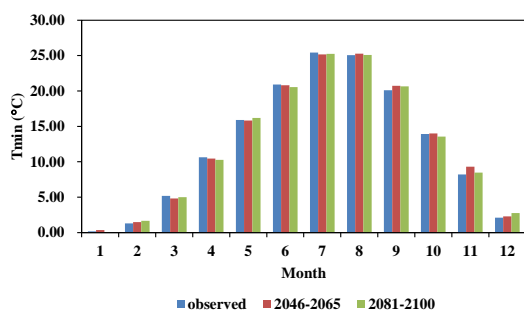
ASD downscaling results revealed that the variation of future precipitation was complex and substantial compared to that of future temperature. *Fig. 6* shows that in the two future periods (2046-2065 and 2081-2100), the majority of months showed an increasing tendency in precipitation. The increase was large in spring and summer (except August), but smaller in other months. Compared to precipitation in 1961-1990, precipitation ranged between -0.3 and 83.6 mm and -5.3 and 89.5 mm in 2046-2065 and 2081-2100, respectively. In general, precipitation in the two future periods will not change significantly. Intra-annual variation was consistent, with reduced precipitation in January, August and December, and increased precipitation in March, May and July.



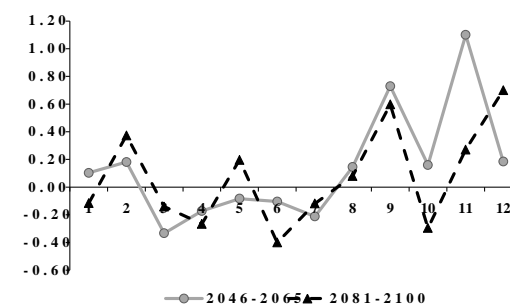
A



B



C



D

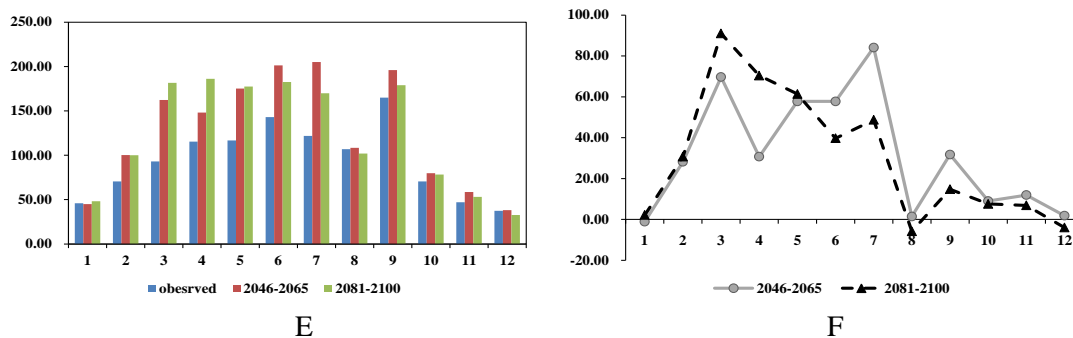


Figure 6. Daily maximum temperature (A-B), minimum temperature (C-D), precipitation (E-F) and their variations in the Taihu basin during two future periods predicted by ASD downscaling model (A, C, and E are comparisons between three elements and their measured values; B, D, and F are monthly changes compared to baseline period)

Response to climate change of water cycle

The authors successfully constructed VIC for the Taihu basin (Liu et al., 2010), which was used in the present study. For meteorological data series under the A1B scenario during the baseline period (1961-1990) generated by the ASD model, including daily precipitation, daily maximum and minimum temperatures, the Thiessen polygon method was used to interpolate the data to $5 \text{ km} \times 5 \text{ km}$ grids, thereby creating climate forcing data. Based on soil and vegetation parameters of the constructed VIC model of the Taihu basin (Liu et al., 2010), the model was run on 1452 grids of the basin, exporting daily runoff depth data at every grid for the period 1961-1990.

Similarly, based on meteorological data series in the future periods (2046-2065 and 2081-2100) generated by ASD, including daily precipitation, daily maximum and daily minimum temperatures, daily runoff depth data at every grid were exported.

Fig. 7 shows monthly changes of runoff depth on each grid for 2046-2065, compared to the baseline period. It is seen that in most areas of the basin, there was a decreasing tendency in monthly runoff depth in the future, of varying magnitude. Areas with large reductions of runoff depth were western Zhejiang and Zhangzhou-Jiaxing-Huzhou; the other areas showed lesser reductions. Particularly, Shanghai showed an increasing tendency during most of the year (January-April and September-December). Western Zhejiang demonstrated a slight increase in runoff depth during flood season.

Fig. 8 shows monthly changes of runoff depth at every grid between 2081-2100 and the baseline period. It is seen that in most areas of the basin, there was a decreasing tendency of monthly runoff depth in the future, with varying magnitude. The runoff depth in the western Zhejiang area tended to decrease compared to the baseline period, but the magnitude of decrease was less than that during 2046-2065. The Yangchengdian area had the largest reduction in runoff depth during March and May, whereas the Hangzhou-Jiaxing-Huzhou area showed a relatively large reduction in winter. Similar to the earlier period of 2046-2065, there was an increasing tendency in Shanghai during most of the year (January-April and October-December).

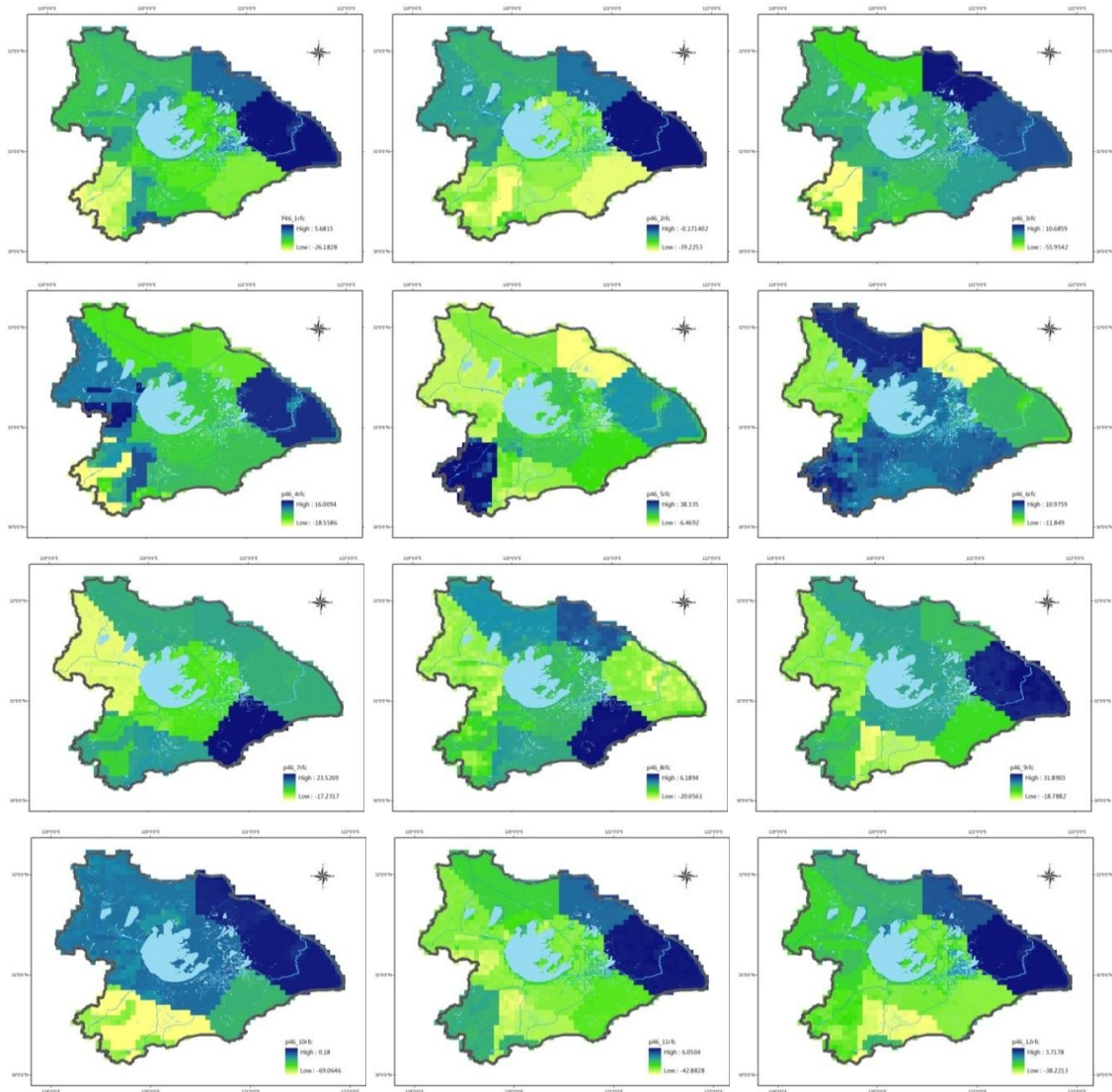


Figure 7. Spatial distribution of monthly runoff depth variation during 2046-2065 under A1B scenario

The Yellow River basin

Construction of future climate change scenario

Based on results of GCM suitability assessment, output data of three GCMs (MRI, CSIRO30, and INM) in the A2 and B1 scenarios were used and underwent interpolation to form $2.5^{\circ} \times 2.5^{\circ}$ grids. The three simulation periods were the same as above. The SDSM model was used for downscaling. Twelve daily predictors were chosen, covering 25 grids in the Yellow River basin. The observation data contained daily precipitation, average temperature, and maximum and minimum temperatures at 79 stations in the basin from 1961 to 1990.

Fig. 9 displays the simulation results of monthly maximum and minimum temperatures from six conditions (three GCMs, each using the A2 and B1 scenarios). It is

seen that both monthly maximum and minimum temperatures had increasing tendencies in most months of the year for all six conditions.

The variation of precipitation was substantially different between conditions (*Fig. 10*). Overall, the CSIRO30 model showed a minimal reduction (monthly variation < 25%) in precipitation, whereas MRI produced the greatest precipitation increase.

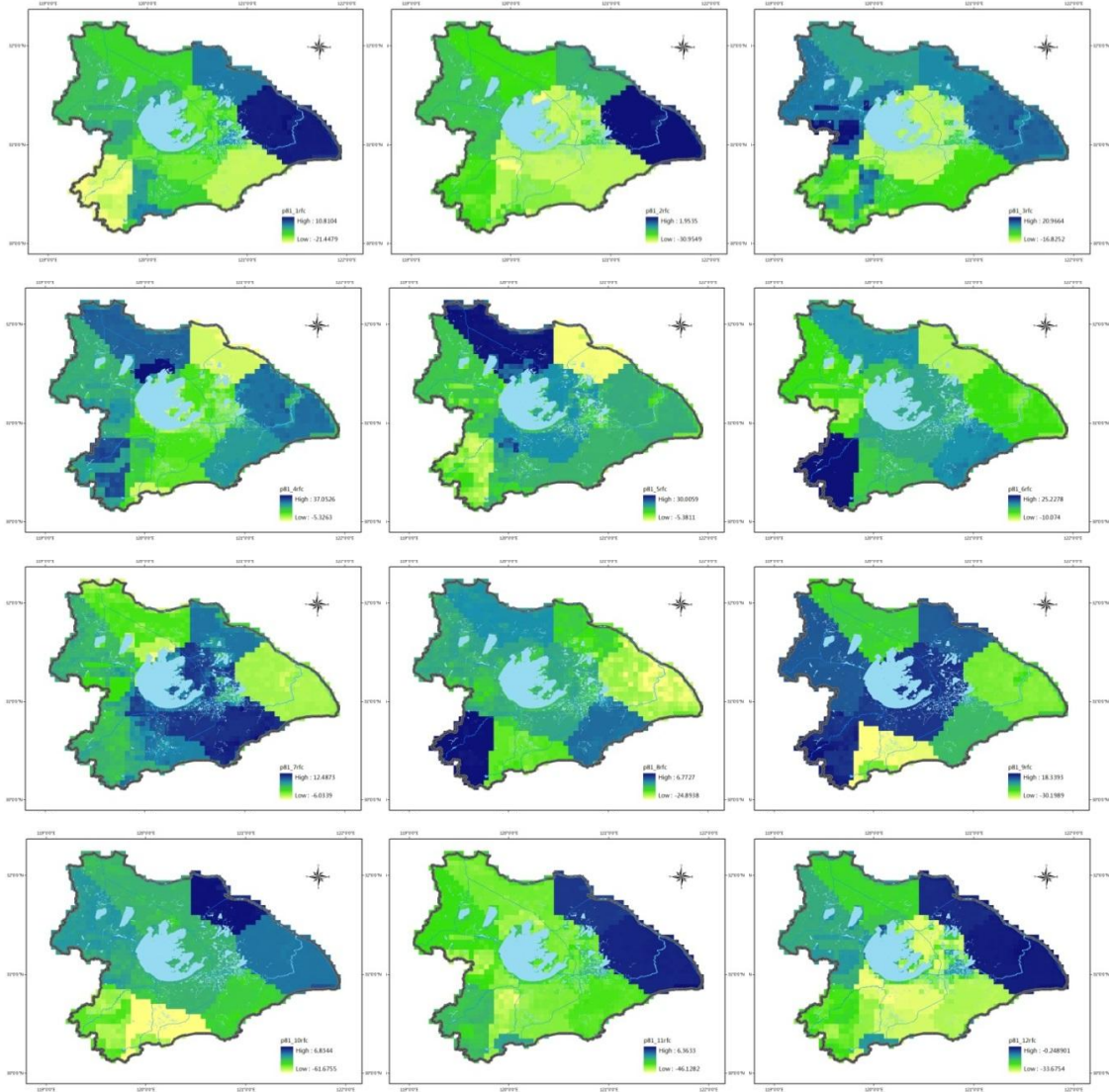
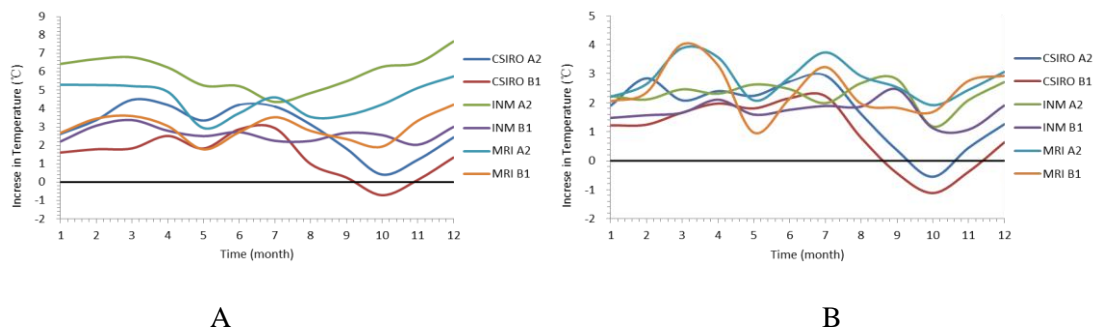


Figure 8. Spatial distribution of monthly runoff depth variation during 2081-2100 under A1B scenario



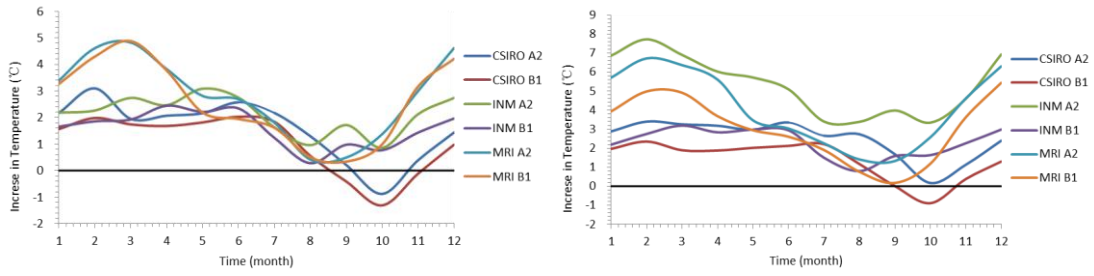


Figure 9. Changes of simulated monthly maximum (A and B) and minimum (C and D) temperature under scenarios A2 and B1 during the period of 2046-2065 and 2081-2100 respectively

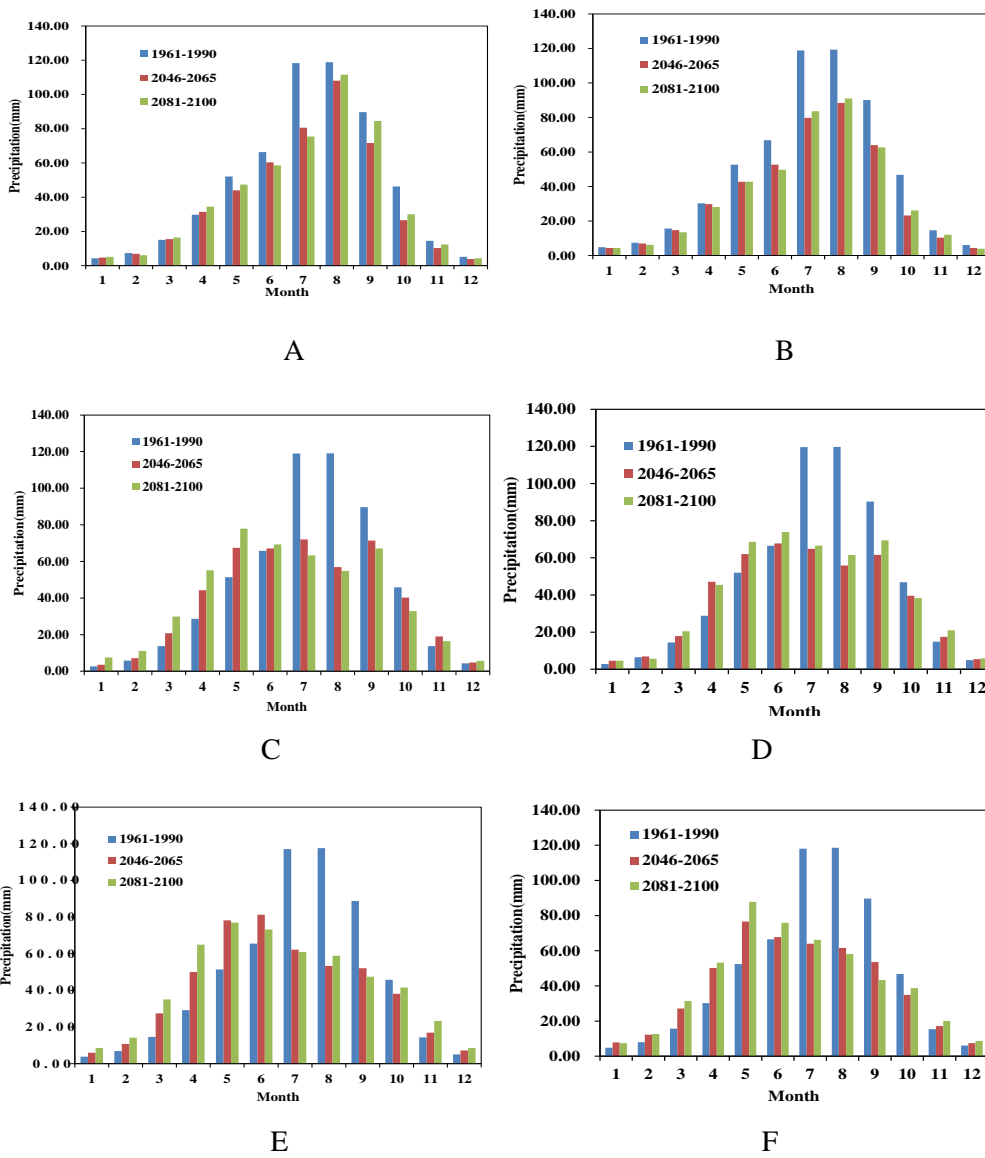


Figure 10. Simulation results of precipitation from three GCMs (A-B: CSIRO30; C-D: INM; E-F: MRI) under various scenarios (a, c, and e: A2; b, d and f: B1)

Response to climate change of water cycle

(1) Construction of distributed hydrological model

The upper reaches of the Yellow River are on the Qinghai-Tibetan Plateau, bordering the Bayan Har Mountains in the south, Qaidam Basin in the north, Kunlun mountains in the west, and Loess Plateau in the east. The geomorphology is alpine grassland. The segment above Lanzhou (hereafter referred to as the upper reaches) has a total length of 2119 km and catchment area of 224,749 km², accounting for 28% of that in the entire basin. *Fig. 11* shows the location of the river basin.

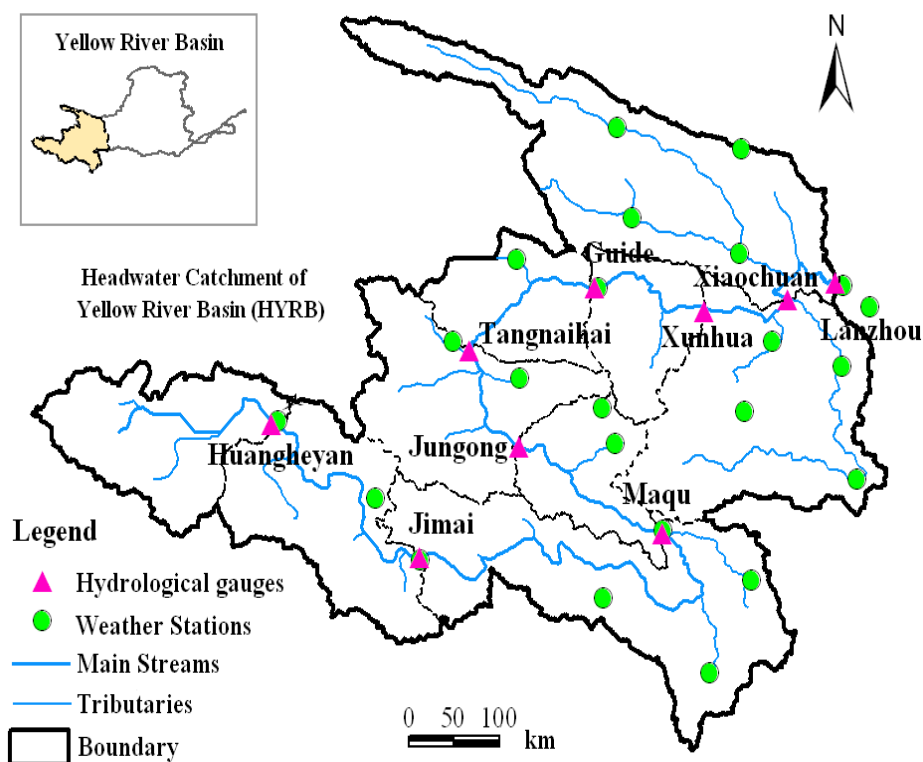
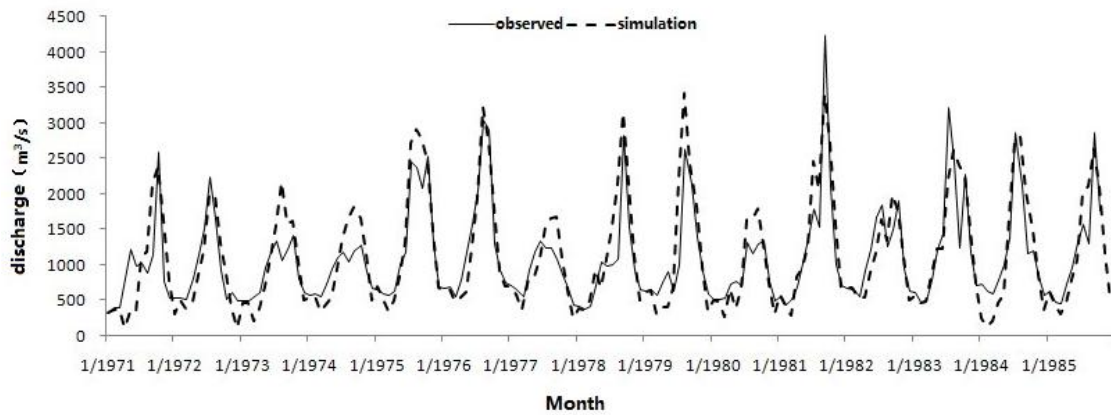
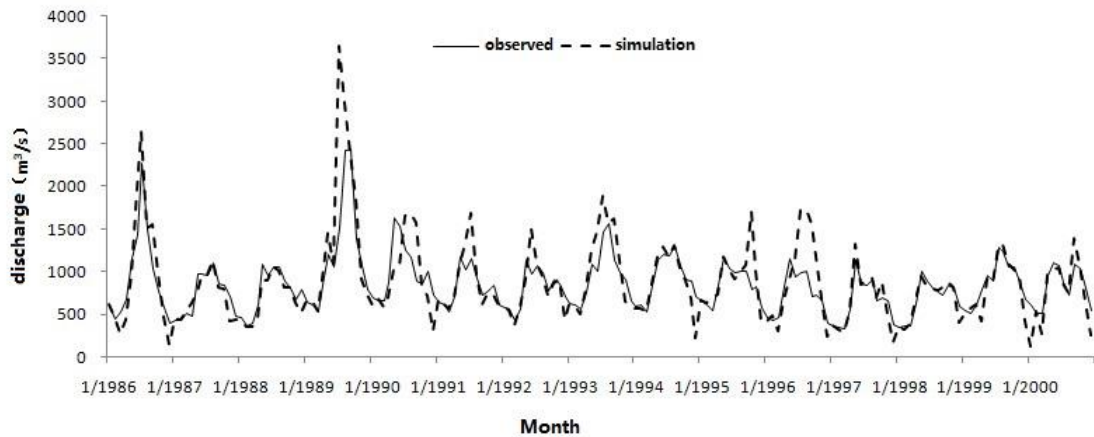


Figure 11. Upper reaches of Yellow River

The SWAT model with the built-in parameter sensitivity analysis module was calibrated and validated during 1971-1985 and 1986-2000, respectively. *Fig. 12* shows a comparison between discharge simulation and measured values at the Lanzhou hydrological station during the calibration and validation periods. In general, model indexes were satisfactory. The Nash-Sutcliffe efficiency and determination coefficients were 0.667 and 0.773 in the calibration period, and 0.626 and 0.709 in the validation period. Hence, the model showed good performance in simulating water balance in the basin.



A



B

Figure 12. Fitted curve of monthly discharge simulation to measured values at Lanzhou hydrological station (A: calibration period; B: validation period)

(2) Response of runoff to future climate change in upper Yellow River basin

Figs. 13-15 present the spatial distribution of mean annual runoff depth during 2046-2065 and 2081-2100 compared to the baseline period, for every sub-basin and downscaling scenarios of the three GCMs. The runoff depth variation of the CSIRO model was -35.8 to 43 mm. In most areas, the variation was between -5 and -20 mm. Overall, the tendency of basin runoff was consistent between different scenario combinations, with runoff decreases in the majority of sub-basins. The area of runoff depth reduction was less under the B1 scenario than that under the A2 scenario. Runoff depth decreased greatly in the Hongyuan, Jiuzhi and Ruorgai areas, generally between -35 and -21 mm. In general, in the downscaling scenario of the CSIRO model, basin runoff depth tended to decrease in most sub-basins.

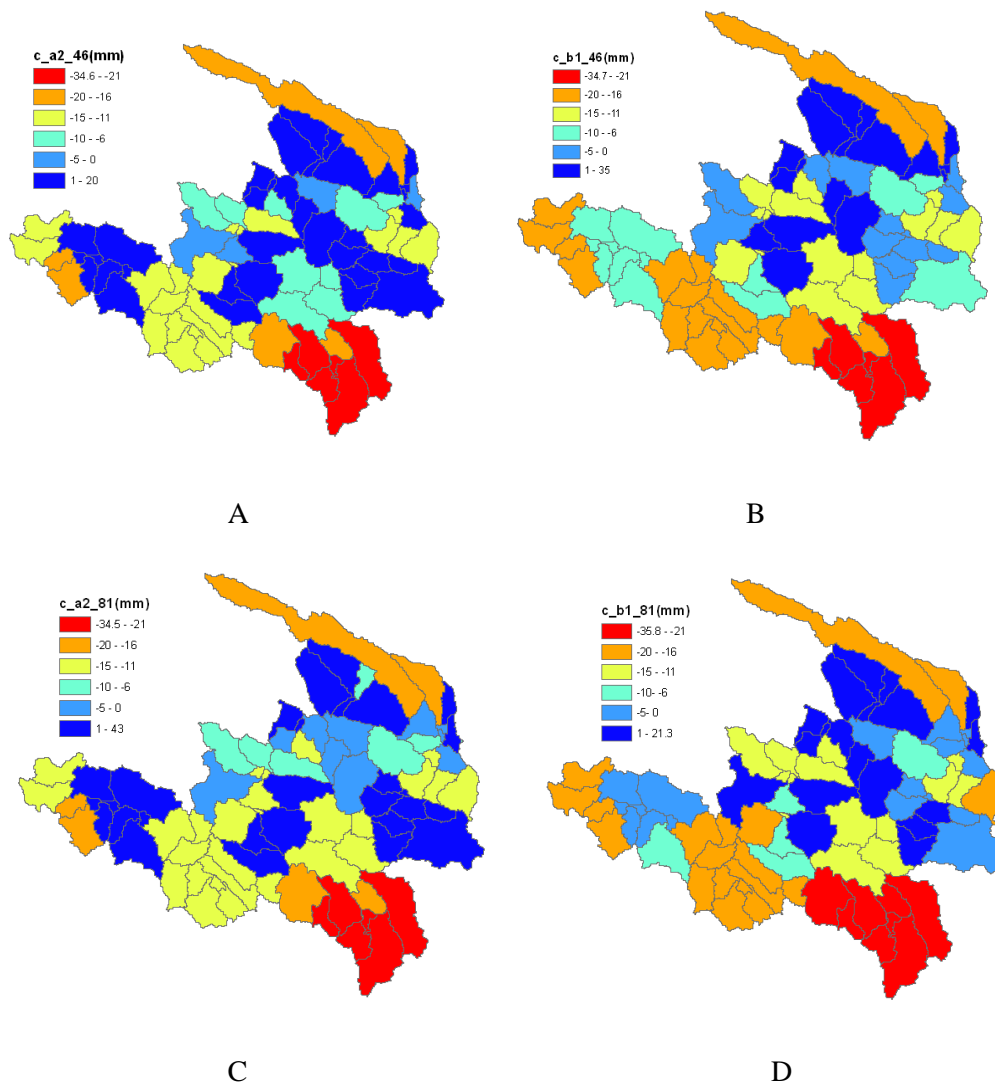


Figure 13. CSIRO-estimated spatial distribution of mean annual runoff depth in sub-basins for 2046-2065 (A and B) and 2081-2100 (C and D) compared to baseline period

For various scenario combinations of the INM model, changes of runoff depth were between -33.9 and 61 mm, with decreases in most sub-basins. The tendency of runoff depth with different scenario combinations was relatively consistent, showing decreasing tendencies (in excess of 20 mm) in southern sub-basins, and mixed increases and decreases in northern sub-basins. Under the A2 emission scenario of INM, the area of sub-basins with reduced runoff during 2081-2100 was larger than that in 2046-2065. Under the B1 scenario, the area was smaller in 2081-2100. The Hongyuan, Jiuzhi, and Ruoergai areas had large reductions in runoff depth, between -31 and -21 mm.

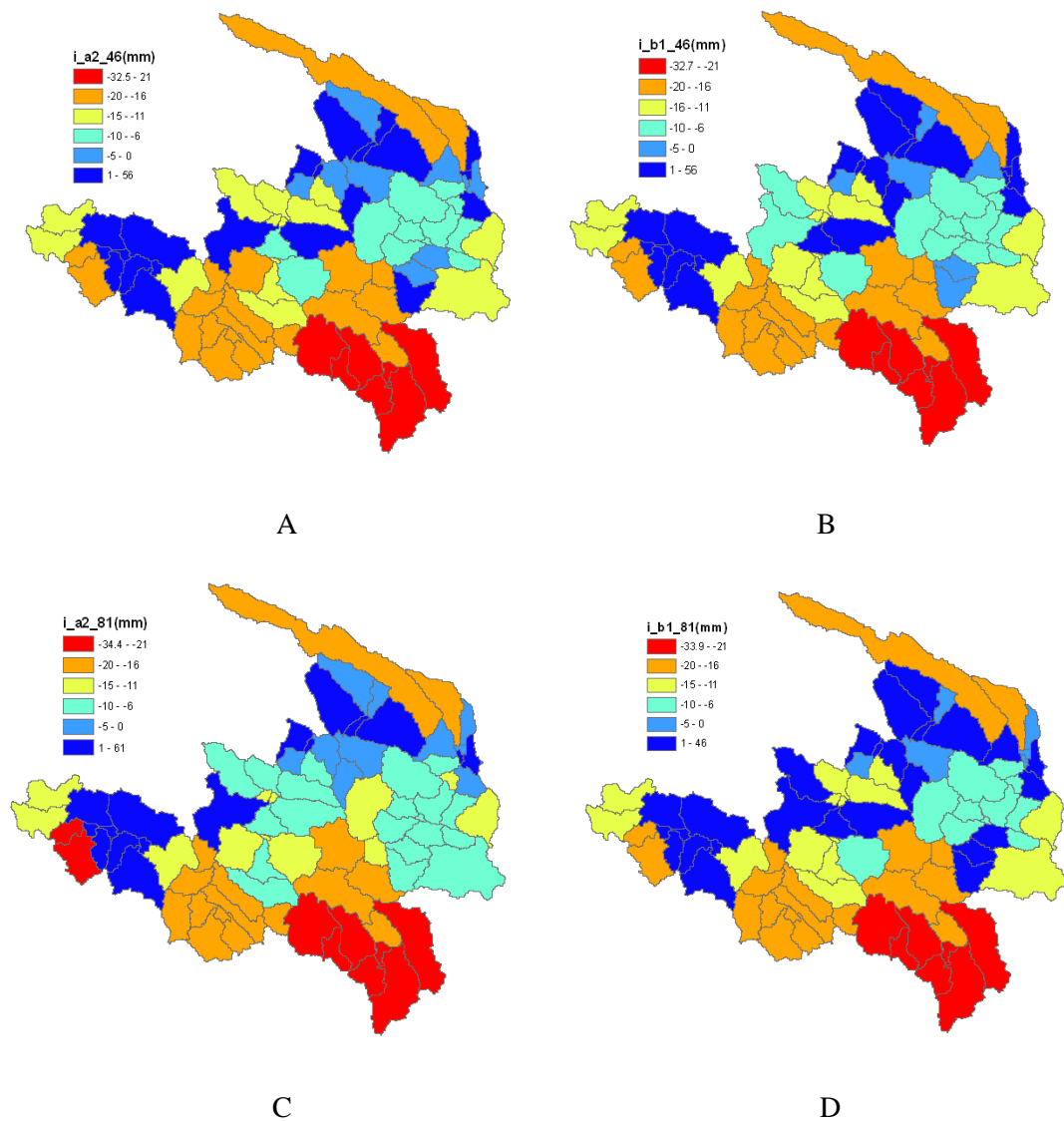


Figure 14. INM-estimated spatial distribution of mean annual runoff depth in sub-basins for 2046-2065 (A and B) and 2081-2100 (C and D) compared to baseline period

For different scenario combinations of the MRI model, runoff depth was between -32.9 and 69 mm, with over half the area of sub-basins showing a decreasing tendency in average runoff depth. In the period 2046-2065, the area of sub-basins with increasing runoff under the A2 scenario was larger than that under the B1 scenario, as was the area with reductions of 16-20 mm. For 2081-2100, the area of sub-basins with increasing runoff under the B1 scenario was larger than that under the A2 scenario, as was the area with reductions of 16-20 mm. The MRI model produced a decreasing tendency in runoff depth over half the basin area. In addition, that depth decreased greatly in Hongyuan, Jiuzhi and Ruergai, generally between -35 and -21 mm.

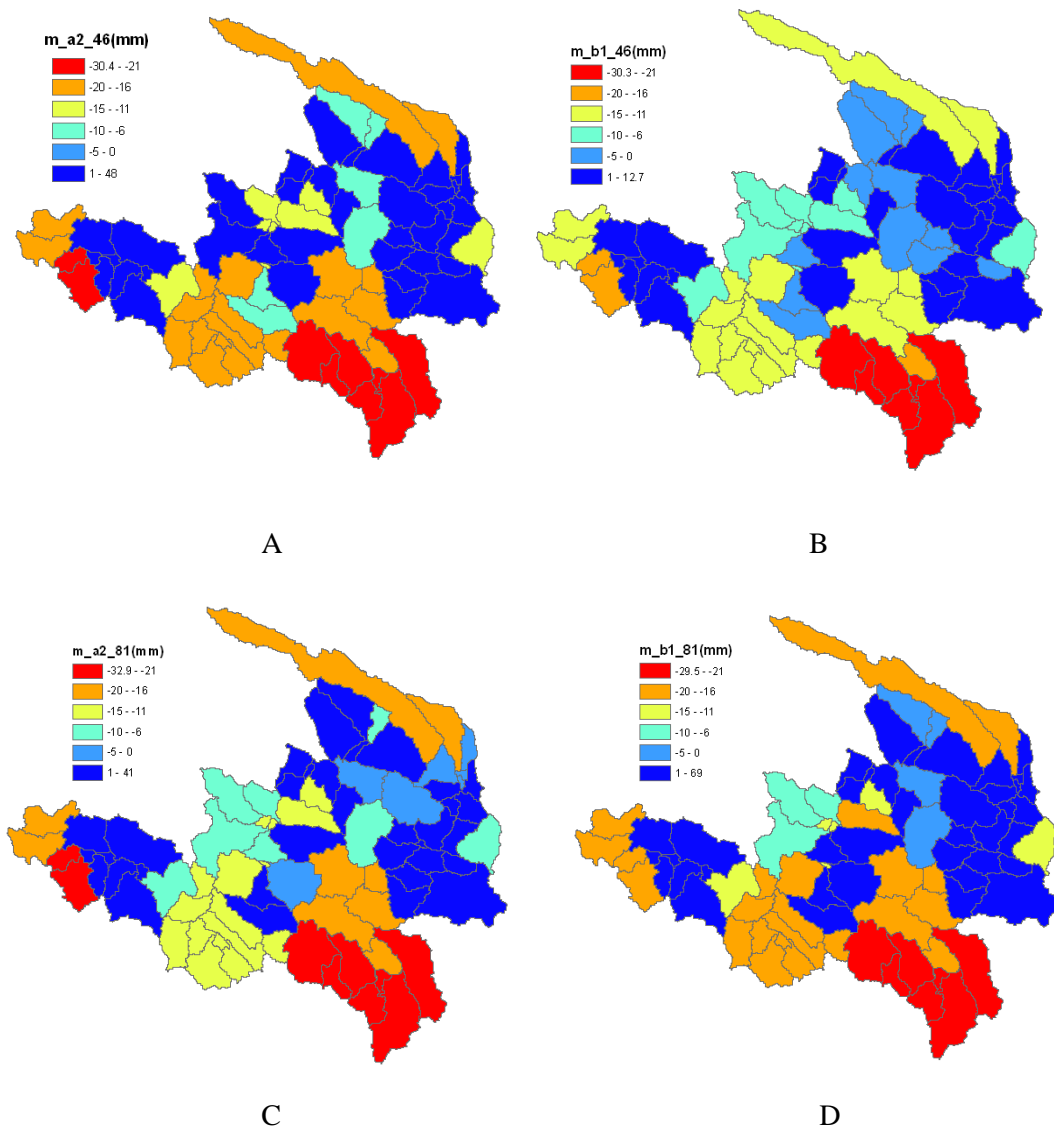


Figure 15. MRI-estimated spatial distribution of mean annual runoff depth in sub-basins for 2046-2065 (A and B) and 2081-2100 (C and D) compared to baseline period

Conclusions

As an important component of the climate system, the water cycle is extremely sensitive to climate change. In the present study, taking the typical areas of the Yangtze and Yellow River basins as objects, we conducted suitability assessments of GCMs and downscaling. Through coupling of GCMs and distributed hydrological models, the impacts of climate change on the river basin water cycle were quantified. The conclusions are as follows.

(1) Based on rank scoring, the degree of fit between statistical values of GCM output and those of reanalysis data was taken as the objective function. Scores were given according to the performance of every objective function, thereby obtaining comprehensive scores for the performance of each GCM in their simulation of the

Yangtze and Yellow River basins. Specifically, the top three models were the MRI, HadGEM1 and INM for the Yangtze River, and FGOALS, ECHAM4 and ECHAM5 for the Yellow River. This indicates a substantial difference between the southern and northern regions of China with respect to the effects of climate change.

(2) Future precipitation and temperature data under the A1B scenario were generated by the ASD downscaling model, which were used to drive the VIC model on 5 km × 5 km grids. Simulation of hydrologic processes in the Taihu basin on the lower reaches of the Yangtze River showed that areas with substantial reduction in runoff depth during 2046-2065 compared to a baseline period were western Zhejiang and Hangzhou-Jiaxing-Huzhou. The western Zhejiang area showed a slight increase in runoff depth during flood season. Runoff depth in western Zhejiang tended to decrease in 2081-2100 compared to the baseline period, but this decrease was less than that during 2046-2065.

(3) The SWAT model gave relatively promising results for the upper reaches of the Yellow River basin. Under the A2 and B1 scenarios, runoff tended to decrease in future periods. In particular, the decrease was greater in 2081-2100 than in 2046-2065. Under different scenario combinations, annual average runoff in 2046-2065 and 2081-2100 was 27.507 and 25.737 billion m³, respectively, reductions of 16.9% and 22.2% compared to the baseline period. Under various scenario combinations, spatial runoff variation in the upper basins of the Yellow River was consistent. In most areas there was a decreasing tendency in runoff depth. Specifically, the decrease was largest in Hongyuan, Jiuzhi and Ruoergai, in excess of 20 mm. Maximum runoff decrease did not vary much with the scenario combination, and was about -30 mm. However, the magnitude of increase was substantially different, between 12.7 and 69 mm.

Acknowledgements. This work was jointly supported by the National Natural Science Foundation of China (51509247, 91425302), and Specialized Research Fund for the Doctoral Program of Higher Education (20130008120005). Assistance from the colleagues in the China Institute of Water Resources and Hydropower Research, Taihu Basin Authority and Chinese Academy of Agricultural Sciences are gratefully acknowledged as well who kindly provided valuable data and advice that greatly improved the quality of the paper.

REFERENCES

- [1] Abdulla, F. A., Lettenmaier, D. P., Wood, E. F., Smith, J. A. (1996): Application of a macroscale hydrologic model to estimate the water balance of the Arkansas-Red River Basin. - *Journal of Geophysical Research Atmospheres* 101: 7449-7459.
- [2] Arnold, J. G., Srinivasan, R., Muttiah, R. S., Williams, J. R. (1998): Large area hydrologic modeling and assessment Part I: Model development. - *Journal of the American Water Resources Association* 34: 73-89.
- [3] Burn, D. H., Sharif, M., Zhang, K. (2010): Detection of trends in hydrological extremes for Canadian watersheds. - *Hydrological Processes* 24: 1781-1790.
- [4] Cao, Y., Zhang, G. H. (2009): Applicability Evaluation of Global Circulation Models in the Yellow River Basin. - *Journal of China Hydrology* 29: 1-5.
- [5] Chen, Z. K. (2002): Sustainable drought and water crisis in North China. - *China Water Resources* 4: 8-11.
- [6] Chu, Q., Xu, Z. X., Jiang, X. H. (2012): Comparison of Two Statistical Downscaling Methods in the Taihu Basin. - *Resources Science* 34: 2323-2336.

- [7] Ding, Y. H., Ren, G. Y. (2008): An introduction to climate change science in China. - Beijing: China Meteorological Press.
- [8] Ding, Y. H., Ren, G. Y., Shi, G. Y., Gong, P., Zheng, X. H., Zhai, P. M., Zhang, D. E., Zhao, Z. C., Wang, S. W., Wang, H. J., Luo, Y., Chen, D. L., Gao, X. J., Dai, X. S. (2006): National Assessment Report of Climate Change (I): Climate change in China and its future trend. - *Advances in Climate Change Research* 2: 3-8.
- [9] Elfert, S., Bormann, H. (2010): Simulated impact of past and possible future land use changes on the hydrological response of the Northern German lowland "Hunte" catchment. - *Journal of Hydrology* 383:245-255.
- [10] Fang, J.Y., Tang, Y.H., Son, Y. (2010): Why are East Asian ecosystems important for carbon cycle research?. - *Science China (Life Science)* 53(7): 753-756.
- [11] Fu, C. B., An, Z. S., Guo, W. D. (2005): Evolution of Life-Supporting Environment in Our Nation and The Predictive Study of Aridification in Northern China (I): Main Scientific Issues and Achievements. - *Advances in Earth Sciences* 20: 1157-1167.
- [12] Hadson, D. A., Jones, R. G. (2002): Regional climate model simulations of present-day and future climates of southern Africa. - Hadley Centre Technical Note 39; Hadley Centre for Climate Prediction and Research, Met Office: London Road, Bracknell, UK.
- [13] Hessami, M., Gachon, P., Ouarda, T. B. M. J., St-Hilaire, A. (2008): Automated regression-based Statistical Downscaling tool. - *Environmental Modelling & Software* 23: 813-834.
- [14] Jeong, J., Kim, H., Chae, D., Kim, E. (2014): The effect of a case-based reasoning instructional model on Korean high school students' awareness in climate change unit. – *Eurasia Journal of Mathematics, Science and Technology Education* 10:427-435.
- [15] Jung, I. W., Chang, H. (2011): Assessment of future runoff trends under multiple climate change scenarios in the Willamette River Basin, Oregon, USA. - *Hydrological Processes* 25: 258-277.
- [16] Karamouz, M., Noori, N., Moridi, A., Ahmadi, A. (2011): Evaluation of floodplain variability considering impacts of climate change. - *Hydrological Processes* 25: 90-103.
- [17] Lin, E. D., Xu, Y. L., Jiang, J. H., Li, Y. E., Yang, X., Zhang, J. Y., Li, C. X., Wu, S. H., Zhao, Z. Q., Wu, J. G., Ju, H., Yan, C. R., Wang, S. R., Liu, Y. F., Du, B. L., Zhao, C. Y., Qin, B. F., Liu, C. Z., Huang, C. Y., Zhang, X. Q., Ma, S. M.. (2006): National Assessment Report of Climate Change (II): Climate change impacts and adaptation. - *Advances in Climate Change Research* 2: 51-56.
- [18] Liu, B. H., Xu, M., Henderson, M., Gong, W. (2004): A spatial analysis of pan evaporation trends in China, 1955-2000. - *Journal of Geophysical Research Atmospheres* 109: 1255-1263.
- [19] Liu, C. M. (2004): Study of some problems in water cycle changes of the Yellow River basin. - *Advances in Water Science* 15: 608-614.
- [20] Liu, C. Z. (2007): The Advances in Studying Detection of Streamflow Trend Influenced by Climate Change. - *Advances in Earth Science* 22: 777-783.
- [21] Liu, L., Xu, Z. X., Huang, J. X. (2010): Impact of Climate Change on Runoff in the Taihu Basin. - *Journal of Beijing Normal University (Natural Science)* 46: 371-377.
- [22] Liu, Q. (2004): Application of the VIC large scale land surface hydrologic model in China. - Ph.D. Dissertation, Hunan University, Changsha, China.
- [23] Liu, Q., McVicar, T. R. (2013): Assessing climate change induced modification of Penman potential evaporation and runoff sensitivity in a large water-limited basin. - *Journal of Hydrology* 464: 352-362.
- [24] Lohmann, D., Raschke, E., Nijssen, B., Lettenmaier, D. P. (1998): Regional scale hydrology: II. Application of the VIC-2L model to the Weser River, Germany. - *Hydrological Sciences Journal* 43: 143-158.
- [25] Marvel, K., Bonfils, C. (2013): Identifying external influences on global precipitation. - *Proceedings of the National Academy of Sciences of the United States of America (PNAS)* 110: 19301-19306.

- [26] Maxino, C. C., Mcavane, B. J., Pitman, A. J., Perkins, S. E. (2008): Ranking the AR4 climate models over the Murray-Darling Basin using simulated maximum temperature, minimum temperature and precipitation. - *International Journal Climatology* 28: 1097-1112.
- [27] Miao, C., Su, L., Sun, Q.H., Duan, Q.Y. (2016): A nonstationary bias-correction technique to remove bias in GCM simulations. - *Journal of Geophysical Research: Atmospheres* 121: 5718–5735.
- [28] Neitsch, S. L., Arnold, J. G., Kiniry, J. R., Williams, J. R. (2005): Soil and Water Assessment Tool Theoretical Documentation Version 2005. - Grassland, Soil and Water Research Laboratory, Agricultural Research Service, Blackland Research Center, Texas Agricultural Experiment Station, Temple, Texas, USA.
- [29] Nijssen, B., Lettenmaier, D. P., Liang, X., Wetzel, S. W., Wood, E. F. (1997): Streamflow Simulation for Continental-Scale River Basins. - *Water Resources Research* 33: 711-724.
- [30] Piao, S., Ciais, P., Huang, Y., Shen, Z. H., Peng, S. S., Li, J. S., Zhou, L. P., Liu, H. Y., Ma, Y. C., Ding, Y. H., Friedlingstein, P., Liu, C. Z., Tan, K., Yu, Y. Q., Zhang, T. Y., Fang, J. Y. (2010): The impacts of climate change on water resources and agriculture in China. - *Nature* 467: 43-51.
- [31] Qian, Z. Y., Shen, G. F., Shi, Y. L. (2007): Several strategic issues related to land and water resource allocation, ecological and environmental protection and sustainable development in Northeast China (comprehensive volume). - Beijing: Science Press.
- [32] Qin, D. H. (2003): Facts, Impact, Adaptation and Mitigation Strategy of Climate Change. - *Bulletin of National Nature Science Foundation of China* 17: 1-3.
- [33] Qin, D. H., Chen, Z. L., Luo, Y., Ding, Y. H., Dai, X. S., Ren, J. W., et al. (2007): Updated Understanding of Climate Change Sciences. - *Advances in Climate Change Research* 3: 63-73.
- [34] Qiu, X. F., Liu, C. M., Zeng, Y. (2003): Changes of pan evaporation in the recent 40 years over the Yellow River Basin. - *Journal of Natural Resources* 18: 437-442.
- [35] Ren, G. Y., Guo, J. (2006): Change in Pan Evaporation and the Influential Factors over China: 1956-2000. - *Journal of Natural Resources* 21: 31-44.
- [36] Stocker, T. F., Qin, D., Plattner, G. K., Tignor, M., Allen, S. K., Boschung, J. (2013): IPCC 2013: Climate Change 2013: The Physical Science Basis. Contribution of Working Group I to the Fifth Assessment Report of the Intergovernmental Panel on Climate Change. - Cambridge University Press: Cambridge, UK.
- [37] Su, F. G., Xie, Z. H. (2003): A model for assessing effects of climate change on runoff in China. - *Progress in Natural Science* 13: 701-707.
- [38] Varis, O., Kajander, T., Lemmelä, R. (2004): Climate and Water: From Climate Models to Water Resources Management and Vice Versa. - *Climatic Change* 66: 321-344.
- [39] Wang, G. Q., Wang, Y. Z., Kang, L. L. (2002): Analysis on the Sensitivity of Runoff in Yellow River to Climate Change. - *Journal of Applied Meteorological Science* 1: 117-121.
- [40] Wang, S. R., Zheng, S. H., Cheng, L. (2003): Studies on Impacts of Climate Change on Water Cycle and Water Resources in Northwest China. - *Climatic and Environmental Research* 8: 43-51.
- [41] Wilby, R. L., Dawson, C. W., Barrow, E. M. (2002): SDSM — A decision support tool for the assessment of regional climate change impacts. - *Environmental Modelling & Software* 17: 145-157.
- [42] Xia, J., Thomas, T., Ren, G. Y., Cheng, X. T., Wang, J. X., Wang, Z. J., Yan, M. C., Liu, X. J., Ian, H. (2008): Potential Impacts of Climate Change on Water Resources in China: Screening for Adaptation and Management. - *Advances in Climate Change Research* 4: 215-219.
- [43] Xu, M., Ma, C. (2009): Yangtze River Basin Climate Change Vulnerability and Adaptation Report. - China Water Power Press, Beijing.
- [44] Xu, Z. X., Liu, L., Liu, Z. F. (2015): Impacts of climate change on river basin water cycle. - Beijing: Science Press.

- [45] Xu, Z. X., Liu, P., Liu, W. F. (2013): Automated statistical downscaling in several river basins of the Eastern Monsoon region, China. - Proceedings of H01, IAHS-IAPSO-IASPEI Assembly,
- [46] Xu. Y., Ding, Y. H., Zhao, Z. C. (2002): Detection and Evaluation of Effect of Human Activities on Climatic Change in East Asia in Recent 30 Years. - Journal of Applied Meteorological Science 13: 513-525.
- [47] Yang, J. P., Ding, Y. J., Chen, H. S., Liu, L. Y. (2003): Variations of Precipitation and Evaporation in North China in Recent 40 Years. Journal of Arid Land Resources & Environment 17: 6-11.
- [48] Ye, D. Z., Huang, R. H. (1996): Pattern and causes of draught and waterlogging in Yellow River and Yangtze River basins. - Jinan: Shandong Science and Technology Press.
- [49] Yuan, F., Xie, Z. H., Ren, L. L., Huang, Q. (2005): Hydrological variation in Haihe River Basin due to climate change. - Journal of Hydraulic Engineering 36: 274-279.
- [50] Zhang, J. Y., Liu, J. F. (2000): A model to evaluate and analyze the effect of climate anomalies on water resources. - Advances in Water Science 11: 1-9.
- [51] Zhang, Q., Xu, C.Y., Yang, T. (2009): Variability of water resource in the Yellow River basin of past 50 years, China. - Water Resources Management 23 (6): 1157-1170.
- [52] Zhang, Y.L., Song, C.H., Zhang, K.R., Cheng, X.L., Bang, L.E., Zhang, Q.F. (2014): Effects of land use/land cover and climate changes on terrestrial net primary productivity in the Yangtze River Basin, China, from 2001 to 2010. - Journal of Geophysical Research: Biogeosciences 119: 1092-1109.
- [53] Zhang, Z. X., Jiang, T., Zhang, J. C., Zhang, Q., Liu, X. F. (2008): Spatial-temporal properties of moisture budget and associated large-scale circulation in the Yangtze River Basin. - Journal Lake Sciences 20: 733-740.
- [54] Zhou, X. X., Ding, Y. H., Wang, P. X. (2008): Moisture transport in Asian summer monsoon region and its relationship with summer precipitation in China. - Acta Meteorologica Sinica 66: 59-70.